Progress in Organic Coatings 195 (2024) 108681

Contents lists available at ScienceDirect

Progress in Organic Coatings

journal homepage: www.elsevier.com/locate/porgcoat

Anti-corrosion peptide coatings and laser patterning for application on flexible transparent silver nanowire electrodes

Andrés Seral-Ascaso [a,b,**], Ruth Lahoz [c], Manoj Tripathi [d], Katrín L. Elídóttir [d], Vicente L. Cebolla [b], Izabela Jurewicz [e], Alan B. Dalton [d], Rosa Garriga [f,*], Edgar Muñoz [b,*]

[a] Archent Nanotechnologies, S.L., Génova 11, 28006 Madrid, Spain
[b] Instituto de Carboquímica (ICB), CSIC, Miguel Luesma Castán 4, 50018 Zaragoza, Spain
[c] Instituto de Nanociencia y Materiales de Aragón (INMA), CSIC-Universidad de Zaragoza, EINA, Edificio Torres Quevedo, María de Luna 3, 50018 Zaragoza, Spain
[d] Department of Physics and Astronomy, University of Sussex, Brighton BN1 9RH, UK
[e] Department of Physics, Faculty of Engineering & Physical Sciences, University of Surrey, Guildford GU2 7XH, UK
[f] Departamento de Química Física, Universidad de Zaragoza, 50009 Zaragoza, Spain

ARTICLE INFO

Keywords:
Peptide coatings
Silver nanowires
Anti-corrosion coatings
Transparent electrodes
Oligoglycine self-assemblies
Laser patterning

ABSTRACT

This work describes physicochemical processing strategies to allow the efficient use of oligoglycine-based coatings for corrosion protection of transparent silver nanowire (AgNW) electrodes fabricated on flexible polyethylene terephthalate (PET) substrates. The peptide anti-corrosion coatings consist of two-dimensional amino-terminated oligoglycine peptide assemblies, denoted as tectomers. Tectomer sheets are hydrophobic in nature and act as moisture barrier and protective layer preventing oxidation and degradation of the nanowires when exposed to atmospheric conditions. Moreover, tectomer coatings markedly decrease the AgNW electrode sheet resistance (R_s) by mechanical squeezing of wire-to-wire junctions in the network. Enhanced adhesion of the tectomer coatings to PET was achieved by a simple hydrolysis process that generates carboxyl and hydroxyl groups on the plastic substrate, enabling a strong interaction with the amino groups on the tectomer surface. R_s values as low as 29.3 Ω/sq with 94.4 % T were achieved for tectomer-coated AgNW electrodes, which are competitive with commercially available AgNW and ITO electrodes. Finally, peptide-coated AgNW networks on PET substrates were efficiently patterned by a one-step laser ablation process without damaging the substrate, offering promise for their use as components in flexible optoelectronics and touchscreen technologies.

1. Introduction

Silver nanowires (AgNWs) have a huge potential in optoelectronics due to their high electrical conductivity, high optical transmittance, and flexibility [1–3]. Thus, much effort is being devoted in recent years to exploit those structural and physical properties to develop AgNW-based solar cells, displays, organic light emitting diodes, flexible transparent electrodes, touch sensors, stretchable pressure sensors, and electromagnetic interference shielding materials, for a wide range of applications in diverse areas including wearable electronics, energy storage and harvesting, touchscreen technologies, electronic skins, and in biomedicine [3–11]. The AgNW-based technology aims to complement and eventually replace indium tin oxide (ITO), the conventional material for the fabrication of highly transparent and conducting electrodes, as ITO inherent brittleness and limited and potentially restricted indium availability pose serious drawbacks for its application in the current demanding field of flexible electronics.

Implementing AgNW-based technologies requires the development of coatings for AgNW corrosion protection: AgNWs readily corrode in air atmosphere mainly due to the presence of trace amounts of hydrogen sulfide and carbonyl sulfide, that lead to silver sulfide formation on the AgNW surface and nanowire shortening and, ultimately, to electrode failure [12]. Films of a variety of materials -including metal oxides [13,14], polymers (such as polyvinyl alcohol (PVA), polyurethane (PU), polymethyl methacrylate (PMMA), polyvinylidene difluoride (PVDF), polyaniline (PANI), and poly(3,4-ethylenedioxythiophene) polystyrene sulfonate (PEDOT:PSS), to name a few) [15–19], epoxy resins [20], sulfur-containing organic compounds [21,22], and graphene materials

* Corresponding authors.
** Correspondence to: A. Seral-Ascaso, Archent Nanotechnologies, S.L.
E-mail addresses: aseral@escyra.es (A. Seral-Ascaso), rosa@unizar.es (R. Garriga), edgar@icb.csic.es (E. Muñoz).

https://doi.org/10.1016/j.porgcoat.2024.108681
Received 2 May 2024; Received in revised form 15 July 2024; Accepted 17 July 2024
Available online 24 July 2024

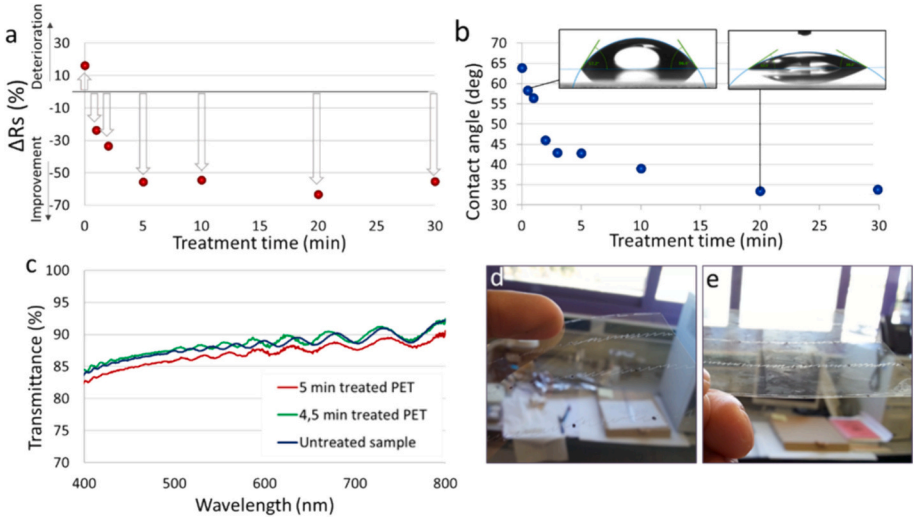

Fig. 1. (a) R_s variation in AgNW/tectomer electrodes as a function of the duration of the PET hydrolysis treatments. The addition of tectomer on AgNW electrodes deposited on pristine, non-functionalized PET substrates did not lead to decreased R_s values but, instead, to increased R_s (data at $t = 0$). (b) Contact angle measurements on PET as a function of the duration of the PET hydrolysis treatments. (c) UV-vis spectra showing the effect on T of the duration of PET hydrolysis treatments. (d) and (e) show pictures of PET after 4.5 and 5 min of treatment, respectively. Note the opacity in (e).

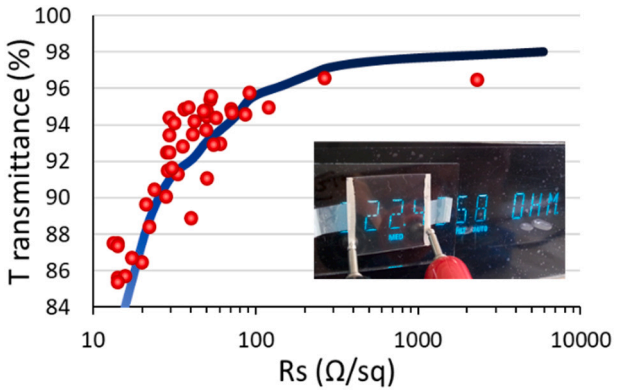

Fig. 2. Transmittance T (%) plotted versus R_s for pristine AgNW electrodes (blue line) and AgNW/tectomer hybrids (red dots). Inset: picture of a AgNW/tectomer electrode with R_s and T values of 22.4 Ω and 88.4 %, respectively. (For interpretation of the references to color in this figure legend, the reader is referred to the web version of this article.)

[23]- have been reported to efficiently act as passivation layers to shield against AgNW corrosion. On the other hand, the application of AgNW electrodes in functional devices require of the use of patterning strategies that enable the fabrication of circuits and interconnects of any desired shape [6,11,24–28].

Amino-terminated oligoglycines consist of short polyglycine chains connected with alkyl linkers. These oligoglycines self-assemble forming two-dimensional structures, typically micrometer sized and 5–6 nm thick, denoted as tectomers, through cooperative hydrogen bonding formation between neighboring polyglycine antennae [29–31]. The remarkable and unique structural and physicochemical features of tectomers combined with their versatile surface chemistry, adhesive properties, and biocompatibility result in remarkable coating capabilities that have been successfully used for the production of novel nanocomposite materials [32], the functionalization of fiber materials and textiles [33], and the development of sensors [34,35]. As an example of the vast potential of these peptide assemblies for the fabrication of functional coatings, in a previous work we reported on the AgNW corrosion protection capabilities of oligoglycine tectomer films: AgNW electrodes deposited on glass substrates were coated with tectomer thin films, so the resulting tectomer coatings not only reduce the AgNW electrode sheet resistance (R_s) by mechanically pushing loosely connected AgNWs, leading to an increased number of inter-wire contacts while keeping the high electrode transparency (transmittance (T) values above 90 %), but also impart increased device hydrophobicity (therefore acting as moisture barriers) and AgNW anti-corrosion functions even under harsh atmospheric conditions (85 °C, 85 % relative humidity) [36], where AgNW corrosion increases considerably [12,20,37–39].

The aim of this work is to further extend this research to the fabrication of flexible, tectomer-coated highly transparent AgNW electrodes that can compete in the marketplace in terms of R_s and T with high performance, commercial AgNW and ITO electrodes. A hydrolysis procedure was applied to flexible polyethylene terephthalate (PET) substrates (a plastic substrate commonly used in bendable optoelectronics) to improve the adhesion of the tectomer anti-corrosion coating. We have also implemented a simple, one-step laser patterning route for the fabrication of interdigitated tectomer-coated AgNW electrodes for their potential integration as components in a variety of optoelectronic devices and wearables, a key issue in electrode prototyping toward device commercialization.

2. Materials and methods

2.1. Materials

Amino-terminated biantennary oligoglycine C_8H_{16}(—CH_2—NH—Gly_4)$_2$·2HCl, purity >95 %, was purchased from PlasmaChem GmbH and used as received. AgNWs, 22.1 nm mean diameter and 21.3 μm on average length (Fig. A.1), 1 wt% in IPA, were supplied by Zhejiang Kechuang Advanced Materials Technology Co., Ltd. (ref. Ink AW020). PET film, 175 μm thick and intrinsic transmittance 87.5 %, was purchased from Goodfellow Cambridge Limited (ref. ES30-FM-000140). Additional experiments were performed using glass microscope slides (Ghäasel). NaOH pellets, purity ≥98 % and HCl (37 % in water) were supplied by Sigma-Aldrich.

2.2. Preparation of tectomer aqueous solutions

1 mg·mL^{-1} oligoglycine solutions in ultrapure water (Siemens LaboStar DI/UV 2 system, resistivity: 18.2 MΩ cm at 25 °C) were prepared

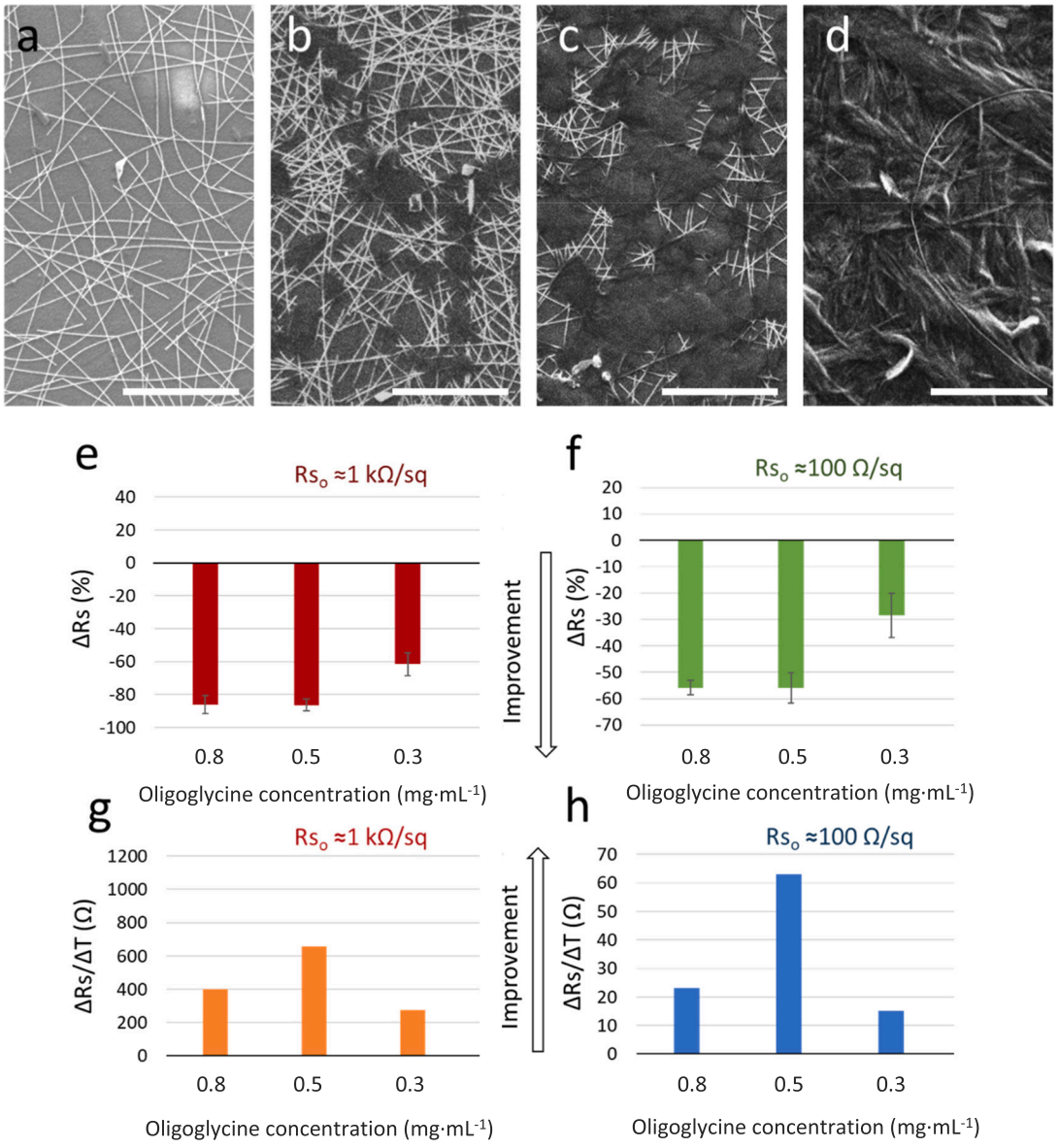

Fig. 3. SEM images of R_{s0} ~100 Ω/sq AgNW networks on PET (a) and after de addition and drying of 50 μL of (b) 0.3 mg·mL^{-1}, (c) 0.5 mg·mL^{-1} and (d) 0.8 mg·mL^{-1} oligoglycine solutions. Scale bar: 3 μm. ΔR_s values after tectomer coating using oligoglycine solutions of the indicated concentrations for electrodes with (e) Rs_0 ~1 kΩ/sq and (f) R_{s0} ~100 Ω/sq. The corresponding $\Delta R_s/\Delta T$ values for electrodes with (g) R_{s0} ~1 kΩ/sq and (h) R_{s0} ~100 Ω/sq.

Table 1
Comparison of the features of tectomer-coated AgNW electrodes fabricated here, and those of some commercially AgNW and ITO electrodes.

	R_s (Ω/sq)	T (%)
Tectomer-coated AgNW electrodes (this work)	29	94
Toray Ag nano-wire film	50-250	90
C3 Nano Activegrid™ film	50	92
ITO (Merck)	30-60	84

Table 2
Optimal laser patterning conditions for AgNW/tectomer electrodes on glass and PET substrates.

Substrate	Intensity (A)	Pulse frequency (kHz)	Beam speed (mm·s^{-1})
Glass	6	150	150
PET	4	60	150

by bath sonication (100 W Branson 2510 bath sonicator) for 10 min. The solutions were prepared and kept at room temperature 40 min before being drop-cast on AgNW electrodes.

2.3. PET hydrolysis

Chemical surface modification of PET was performed to yield carboxylic and hydroxyl groups on the surface [40–42] in order to enhance tectomer adhesion to PET substrates. 72 × 80 mm PET sheets were placed floating on 4 M NaOH solutions at 330 K and, consequently, only one side of the PET substrates was functionalized. The sheets were removed after 270 s, then immersed in 0.5 M HCl solutions for 3 s to rinse off NaOH, and finally washed with ultrapure water for 10 s and dried to yield hydrolyzed PET films.

2.4. AgNW electrode preparation

The hydrolyzed PET films were cut into 18 × 20 mm pieces. 1 mm

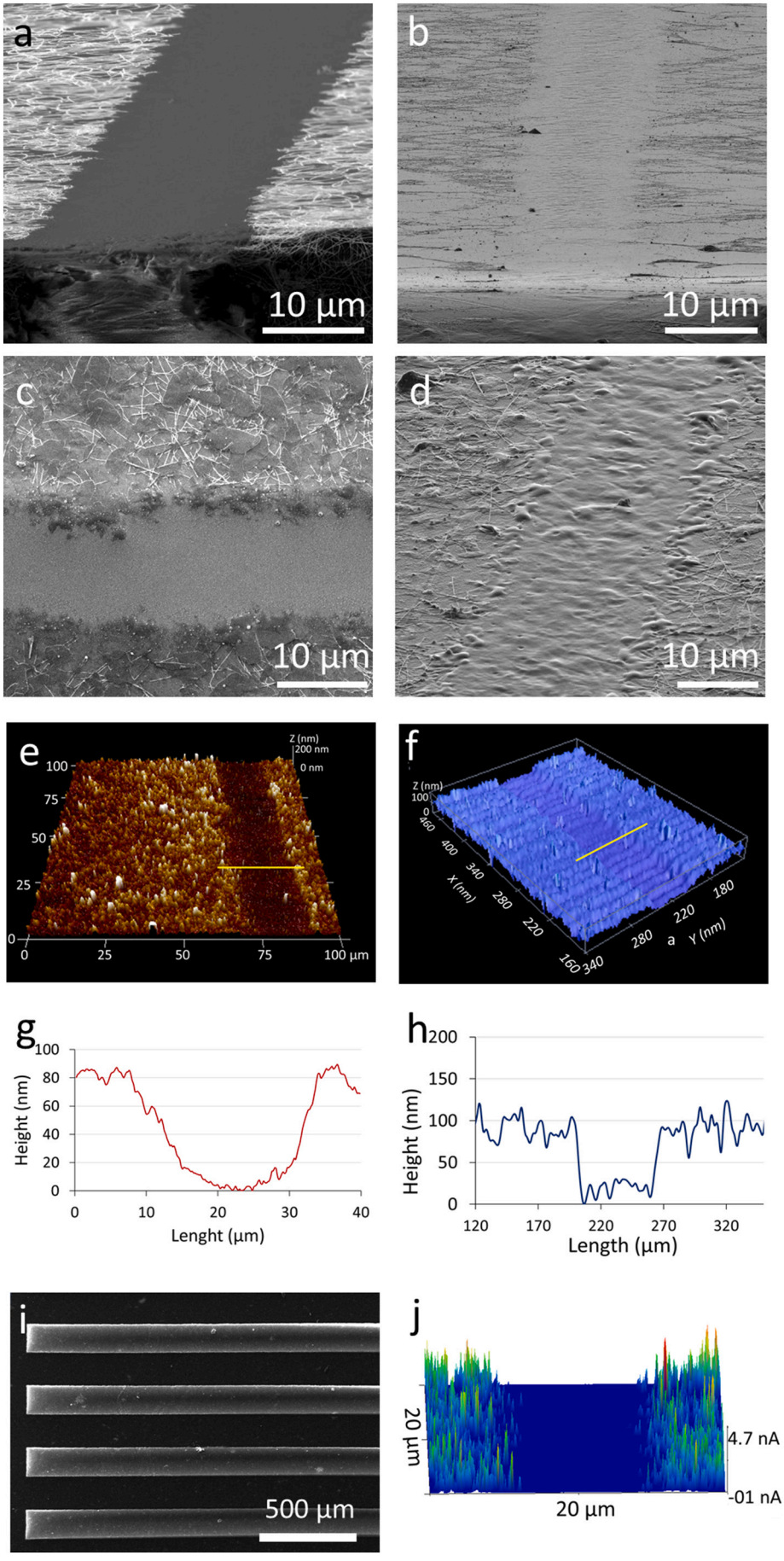

(caption on next page)

Fig. 4. SEM images of laser ablated AgNW electrodes on (a) glass and (b) PET supports. SEM micrographs of laser ablated AgNW/tectomer electrodes on (c) glass (top-view) and (d) PET (tilted-view). 3D AFM topography (e) and height profile (g) of a laser patterned line of a AgNW/tectomer electrode on glass. Confocal microscopy image of the topography of a laser patterned line on a AgNW/tectomer electrode on PET (f) and height profile (h). SEM image of a patterned AgNW/tectomer electrode on PET, mimicking commercial interdigitated electrodes (i). Conductive AFM image showing the electrically insulating characteristics of the paths fabricated by laser patterning (j).

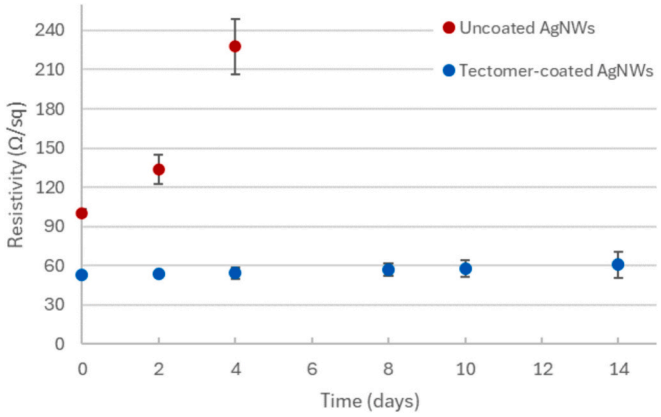

Fig. 5. Corrosion study of highly transparent (94 % T) tectomer-coated AgNW electrodes on PET supports, treated in a built-in-house controlled humidity chamber (40 % RH) at 60 °C in the dark for 2 weeks, compared to uncoated AgNW electrodes.

wide electrical contacts were painted on opposite sides of the tested electrodes using Ag paint, so the final electrodes, without considering the Ag paint, consisted of 18 × 18 mm squares. Then, 0.05 mg·mL^{-1} AgNW dispersions in IPA were sprayed on the substrate with an airbrush operated at 6 bar until the set R_s value was measured.

2.5. Tectomer deposition on AgNW electrodes

50 μL of 0.3, 0.5 and 0.8 mg·mL^{-1} oligoglycine solutions were drop-cast on the AgNW electrodes and then evenly spread over the electrode surface and allowed to dry under ambient conditions.

2.6. Electrode characterization studies

Scanning electron microscopy (SEM) and energy dispersive X-ray spectroscopy (EDX) characterization studies were performed with an Inspect F50 field emission SEM microscope (FEI). Samples were coated with a 14 nm thick Pd layer by sputtering for SEM characterization. Transmission electron microscopy (TEM) micrographs were collected with a FEI Tecnai T20 microscope equipped with a LaB_6 electron gun and operating at 200 KV. Contact angle measurements were performed using a KRÜSS Drop Shape Analyzer DSA 100 system. R_s values were calculated from two-probe electrical resistance measurements performed using a Keithley 2000 multimeter. T values were measured from spectra collected using a Shimadzu 2501PC UV-vis spectrophotometer. R_s and T values shown here correspond to the mean average calculated from 8 independent experiments.

2.7. Laser patterning

Laser patterning experiments were performed using a commercial 2 W Q-switched Yb:YAG diode-pumped pulsed fiber laser (Rofin PowerLine S3 SHG, Germany), operating at 532 nm. The used laser pulse frequency ranged from 20 to 100 kHz while the pulse duration varied from 4 to 100 ns. A CAD software-controlled galvanometric beam steering system enabled precise and repeatable patterns of the desired shape and size.

The patterned electrodes were characterized by SEM, optical confocal microscopy (Sensofar, PLμ2300 model), and conductive atomic force microscopy (AFM, Bruker ScanAsyst microscope, using Pt/Ir-coated Bruker PFTUNA conductive probes).

2.8. Corrosion tests

AgNW electrodes with and without tectomer coating were exposed to harsh atmospheric conditions (60 °C and 40 % relative humidity, RH) by placing them in a custom-made humidity chamber, and their R_s values were measured every 2 days for 2 weeks.

3. Results and discussion

3.1. Chemical surface modification of PET

Peptide/surface interactions are in general very specific and substrate-dependent [43,44]. The surface amino groups of tectomers strongly interact with hydrophilic mica and glass surfaces [29–31], as well as with nanomaterials and surfaces functionalized with carboxylic acid, hydroxy or epoxy groups through hydrogen bonding formation [32,33]. Initial studies on the fabrication of AgNW electrodes on pristine, non-functionalized PET substrates indicated no improvement in the measured R_s values upon addition of tectomer coatings (actually, increased R_s values were measured, see Fig. 1a results at $t = 0$), indicating low tectomer affinity to pristine PET. In order to enhance the adhesion of tectomers to PET substrates and, therefore, to increase the number of wire-to-wire contacts and reduce R_s values, a chemical functionalization procedure was conducted which resulted in carboxylic and hydroxyl groups on the PET surface (Section 2.3). Fig. 1a shows the improvement of the electrical conductivity (as resistivity variation, ΔR_s %) as a function of the duration of PET treatment. For samples treated up to 5 min there is a sharp, time-dependent R_s decrease, until a ΔR_s plateau is reached for longer PET hydrolysis treatments.

Contact angle measurements confirmed PET surface functionalization by a sharp increase in PET hydrophilicity during the first minutes of treatment. Thus, Fig. 1b shows that contact angle values of ultrapure water droplets on functionalized PET decrease as a function of hydrolysis treatment duration, reaching a minimum value in samples treated for 20 min, and then do not change for a longer treatment duration up to 1 h.

With the aim of fabricating highly transparent electrodes, it is required that the hydrolysis treatment does not alter PET optical properties. AFM characterization studies reveal that roughness increases as a function of PET chemical treatment duration (Fig. A.2). Prolonged hydrolysis treatments eventually cause the detachment of small fragments of the polymer, thus turning the smooth, transparent PET surface into a rougher, partially opaque surface, as previously described by Liu et al. [40]. T measurements and optical pictures of hydrolyzed PET sheets show that significant haze and surface damage begins after being treated for 5 min (Fig. 1c-e). Thus, while no significant change in T (only 0.2 % at $\lambda = 550$ nm) occurs for PET substrates treated for up to 4.5 min, T values decrease 1.6 % at $\lambda = 550$ nm after 5 min treatment (Fig. 1c). Therefore, 4.5 min was set as the optimum treatment time to maximize the PET/tectomer interaction.

3.2. Tectomer coating optimization

Fig. 2 shows T as a function of R_s for pristine AgNW electrodes and tectomer-coated AgNW electrodes fabricated, as described in Sections

2.4 and 2.5, respectively.

While the addition of tectomer coatings reduces the R_s of AgNW electrodes, an excess of tectomer thickness would be detrimental for the electrodes' optical properties. Thus, the parameter $\Delta R_s/\Delta T$, defined as the decrease of R_s per unit of decrease in T, is useful for setting the optimum tectomer coating amount in order to decrease R_s while retaining the electrodes' high transparency.

Fig. 3a-d show SEM characterization of pristine AgNW and AgNW/tectomer electrodes fabricated by drop-casting 50 μL of 0.3, 0.5 and 0.8 $mg{\cdot}mL^{-1}$ oligoglycine solutions. Fig. 3e-h show ΔR_s and $\Delta R_s/\Delta T$ values of the electrodes as a function of the amount of deposited tectomer, whose AgNW densities provided initial resistivity (R_{s0}) values of ~1 kΩ/sq and ~100 Ω/sq. According to these results, 0.5 $mg{\cdot}mL^{-1}$ solutions provided the optimal $\Delta R_s/\Delta T$ values (note that, although the R_s improvement achieved is similar to that for 0.8 $mg{\cdot}mL^{-1}$, 0.5 $mg{\cdot}mL^{-1}$ oligoglycine solutions provided higher transparency, resulting in higher $\Delta R_s/\Delta T$ values).

For comparison purposes, AgNWs were further sprayed to provide R_s values similar to those achieved by the addition of 0.5 $mg{\cdot}mL^{-1}$ of oligoglycine solution. For Rs_0 ~1 kΩ/sq, the obtained $\Delta R_s/\Delta T$ value for this AgNW electrode was higher ($\Delta R_s/\Delta T = 972$ Ω) than for the AgNW/tectomer electrode ($\Delta R_s/\Delta T = 650$ Ω, Fig. 3g), meaning that this further addition of AgNWs rapidly increases the electrodes' conductivity (R_s varied from 1124 to 210 Ω/sq) with little change in T. However, this result is not relevant, as R_s values ~210 Ω/sq are too large for high-tech optoelectronics. However, for Rs_0 ~100 Ω/sq, the addition of AgNW resulted in $\Delta R_s/\Delta T = 22$ Ω, which is lower than that of AgNW/tectomer ($\Delta R_s/\Delta T = 63$ Ω, Fig. 3h), meaning that tectomer coatings provide improved performance in this range of R_s. It must be highlighted here that R_s values as low as 29.3 Ω/sq with 94.4 % T were achieved for tectomer-coated AgNW electrodes (in contrast to 91.1%T for electrodes with the same R_s fabricated from AgNWs only), being tectomer-coated AgNW electrodes competitive with commercially available AgNW and ITO electrodes (Table 1).

3.3. Laser patterning of AgNW/tectomer electrodes

Laser processing technology is a convenient tool for patterning metal nanowire electrodes [25,28,45]. In this work, the AgNW/tectomer electrodes both on glass and PET supports were processed with a Q-switched Yb:YAG laser ($\lambda = 532$ nm), to produce electrically insulating scribes necessary for electrode fabrication in touchscreen sensor devices.

Laser patterning parameters (intensity, beam speed, pulse frequency and width, and number of passes) were firstly optimized (Table 2) to create non-conductive paths in the AgNWs electrodes on both glass (Fig. 4a) and PET (Fig. 4b), so AgNWs were removed without damaging the substrates, that could be detrimental to the transparency of the electrode. Then, laser parameters were tuned (Table 2) to create paths in tectomer-coated AgNW electrodes (Fig. 4c, d). Interestingly, AgNWs were observed to present a much lower laser ablation threshold than the tectomer coatings and the substrates. Therefore, it is possible to selectively remove the AgNWs leaving the tectomer coating unaffected, when conveniently tuning the laser parameters, as shown in Fig. A.3. However, the complete removal of AgNWs and tectomer was preferred in order to achieve optimal T values for the electrodes.

AFM and confocal microscopy studies showed that the width of the lines ranged from 15 to 50 nm (Fig. 4e-h). Tectomer-coated AgNW electrodes were patterned mimicking commercial interdigitated electrodes (Fig. 4i). Moreover, conducting AFM characterization confirmed the insulating nature of the laser-ablated paths and, therefore, the resulting complete AgNW removal (Fig. 4j).

3.4. Moisture barrier properties of tectomer coatings for AgNW networks

The performance of AgNW transparent electrodes is closely related to AgNW degradation. High humidity associated with high temperature greatly accelerate the failure of AgNW electrodes [46]. Our previous studies showed that tectomer coatings on AgNW electrodes on glass supports provide outstanding temperature and moisture barrier protection under harsh conditions (85 °C, 85 % RH) [36]. Fig. 5 shows that the R_s of highly transparent (94 % T) AgNW/tectomer electrodes on PET supports, treated at 60 °C under 40 % RH for 2 weeks, only changed from 53 to 60 Ω/sq (11 % increase). In contrast, Fig. 5 also reveals that uncoated AgNW electrodes suffered massive degradation under these conditions.

4. Conclusions

In this work, tectomer-coated transparent and flexible AgNW electrodes on PET substrates have been developed. Chemical functionalization of PET surface by a simple hydrolysis process enhanced tectomer adhesion to the plastic substrate, which favors mechanical squeezing of wire-to-wire junctions in AgNW network, enabling R_s values as low as 29.3 Ω/sq with 94.4 % T, which are competitive with those of commercially available AgNW and ITO electrodes.

Furthermore, tectomer-coated electrodes both on PET and glass substrates have been successfully patterned using a fast, one-step laser ablation process to produce electrically isolated scribes suitable for touchscreen sensor applications.

Protecting AgNW electrodes from environmental factors is a key issue to improve their durability and stability for practical applications. Tectomer coatings efficiently impart anti-corrosion protection to AgNW electrodes even under harsh ambient conditions. It is also known that UV radiation shortens the lifetime and limits the performance of AgNW electrodes [20]. The anti-UV protection properties of tectomers were previously reported elsewhere [31], so future work will consider exploring how tectomer coatings prevent UV-induced AgNW electrode degradation.

CRediT authorship contribution statement

Andrés Seral-Ascaso: Writing – original draft, Supervision, Investigation. **Ruth Lahoz:** Methodology, Investigation. **Manoj Tripathi:** Methodology, Investigation. **Katrín L. Elídóttir:** Methodology, Investigation. **Vicente L. Cebolla:** Supervision, Project administration. **Izabela Jurewicz:** Supervision, Project administration, Conceptualization. **Alan B. Dalton:** Supervision, Project administration, Conceptualization. **Rosa Garriga:** Writing – review & editing, Writing – original draft, Supervision, Project administration, Conceptualization. **Edgar Muñoz:** Writing – review & editing, Writing – original draft, Supervision, Project administration, Conceptualization.

Declaration of competing interest

The authors declare that they have no known competing financial interests or personal relationships that could have appeared to influence the work reported in this paper.

Data availability

The data that support the findings of this study are available within the article. Additional data will be made available on request.

Acknowledgements

This work was funded by Archent Nanotechnologies, S.L. Authors acknowledge the use of instrumentation as well as the technical advice provided by the National Facility ELECMI ICTS, node "Laboratorio de Microscopías Avanzadas (LMA)" at "Universidad de Zaragoza". The authors acknowledge additional support from the Aragón regional government (project E25_23R) and BeAble Capital SGEIC, S.A.

Appendix A. Supplementary data

Supplementary data to this article can be found online at https://doi.org/10.1016/j.porgcoat.2024.108681.

References

[1] S. De, T.M. Higgins, P.E. Lyons, E.M. Doherty, P.N. Nirmalraj, W.J. Blau, J. J. Boland, J.N. Coleman, Silver nanowire networks as flexible, transparent, conducting films: extremely high DC to optical conductivity ratios, ACS Nano 3 (2009) 1767–1774, https://doi.org/10.1021/nn900348c.

[2] M.S. Miller, J.C. O'Kane, A. Niec, R.S. Carmichael, T.B. Carmichael, Silver nanowire/optical adhesive coatings as transparent electrodes for flexible electronics, ACS Appl. Mater. Interfaces 5 (2013) 10165–10172, https://doi.org/10.1021/am402847y.

[3] P.M. Martinez, A. Ishteev, A. Fahimi, J. Velten, I. Jurewicz, A.B. Dalton, S. Collins, R.H. Baughman, A.A. Zakhidov, Silver nanowires on carbon nanotube aerogel sheets for flexible, transparent electrodes, ACS Appl. Mater. Interfaces 11 (2019) 32235–32243, https://doi.org/10.1021/acsami.9b06368.

[4] A.B.V. Kiran Kumar, C.W. Bae, L. Piao, S.-H. Kim, Silver nanowire based flexible electrodes with improved properties: high conductivity, transparency, adhesion and low haze, Mater. Res. Bull. 48 (2013) 2944–2949, https://doi.org/10.1016/j.materresbull.2013.04.035.

[5] M. Cann, M.J. Large, S.J. Henley, D. Milne, T. Sato, H. Chan, I. Jurewicz, A. B. Dalton, High performance transparent multi-touch sensors based on silver nanowires, Mater. Today Comm. 7 (2016) 42–50, https://doi.org/10.1016/j.mtcomm.2016.03.005.

[6] S. Liu, S. Ho, F. So, Novel patterning method for silver nanowire electrodes for thermal-evaporated organic light emitting diodes, ACS Appl. Mater. Interfaces 8 (2016) 9268–9274, https://doi.org/10.1021/acsami.6b00719.

[7] K.-S. Kim, S.O. Kim, C.J. Han, D.U. Kim, J.S. Kim, Y.-T. Yu, C.-R. Lee, J.-W. Kim, Revisiting the thickness reduction approach for near-foldable capacitive touch sensors based on a single layer of Ag nanowire-polymer composite structure, Compos. Sci. Tech. 165 (2018) 58–65, https://doi.org/10.1016/j.compscitech.2018.06.016.

[8] J. Wang, J. Jiu, M. Nogi, T. Sugahara, S. Nagao, H. Koga, P. He, K. Suganuma, A highly sensitive and flexible pressure sensor with electrodes and elastomeric interlayer containing silver nanowires, Nanoscale 7 (2015) 2926–2932, https://doi.org/10.1039/C4NR06494A.

[9] X. Yu, X. Liang, T. Zhao, P. Zhu, R. Sun, C.-P. Wong, Thermally welded honeycomb-like silver nanowires aerogel backfilled with polydimethylsiloxane for electromagnetic interference shielding, Mater. Lett. 285 (2021) 129065, https://doi.org/10.1016/j.matlet.2020.129065.

[10] T.-W. Lee, S.-E. Lee, Y.G. Jeong, Highly effective electromagnetic interference shielding materials based on silver nanowire/cellulose papers, ACS Appl. Mater. Interfaces 8 (2016) 13123–13132, https://doi.org/10.1021/acsami.6b02218.

[11] M.D.S.L. Wimalananda, J.-K. Kim, J.-M. Lee, Patterning of silver nanowire for grid formation by using ultrasonic assisted T clean chemical etching for the application of high transparent electrode, Mater. Sci. Eng. B 228 (2018) 67–73, https://doi.org/10.1016/j.mseb.2017.11.014.

[12] J.L. Elechiguerra, L. Larios-Lopez, C. Liu, D. Garcia-Gutierrez, A. Camacho-Bragado, M.J. Yacaman, Corrosion at the nanoscale: the case of silver nanowires and nanoparticles, Chem. Mater. 17 (2005) 6042–6052, https://doi.org/10.1021/cm051532n.

[13] S. Yu, X. Liu, H. Dong, X. Wang, L. Li, Flexible high-performance SnO_2/AgNWs bilayer transparent conductors for flexible transparent heater applications, Ceram. Int. 47 (2021) 20379–20386, https://doi.org/10.1016/j.ceramint.2021.04.046.

[14] S. Yu, X. Liu, M. Wu, H. Dong, X. Wang, L. Li, All-solution-processed molybdenum oxide-encapsulated silver nanowire flexible transparent conductors with improved conductivity and adhesion, ACS Appl. Mater. Interfaces 13 (2021) 14470–14478, https://doi.org/10.1021/acsami.0c22324.

[15] H. Ha, J.Y. Cheong, T.G. Yun, B. Hwang, Polymeric protection for silver nanowire-based transparent conductive electrodes: performance and applications, Inorganics 11 (2023) 409, https://doi.org/10.3390/inorganics11100409.

[16] G. Li, J. Zhao, Z. Wang, X. Yu, T. Zhao, X. Liang, R. Sun, L. Cao, P. Zhu, Ultrathin, flexible, conductive silver nanowires@polyvinyl alcohol composite film fabricated via the combination of air plasma treatment and thermal sintering for electromagnetic interference shielding, Mater. Lett. 325 (2022) 132814, https://doi.org/10.1016/j.matlet.2022.132814.

[17] S. Yu, X. Ma, X. Li, J. Li, B. Gong, X. Wang, Enhanced adhesion of Ag nanowire based transparent conducting electrodes for application in flexible electrochromic devices, Optical Mater. 120 (2021) 111414, https://doi.org/10.1016/j.optmat.2021.111414.

[18] D.Y. Choi, H.W. Kang, H.J. Sung, S.S. Kim, Annealing-free, flexible silver nanowire–polymer composite electrodes via a continuous two-step spray-coating method, Nanoscale 5 (2013) 977–983, https://doi.org/10.1039/c2nr32221h.

[19] K.-W. Kim, S.B. Lee, S.H. Kim, H.C. Moon, Spray-coated transparent hybrid electrodes for high-performance electrochromic devices on plastic, Org. Electron. 62 (2018) 151–156, https://doi.org/10.1016/j.orgel.2018.07.033.

[20] J. Jiu, J. Wang, T. Sugahara, S. Nagao, M. Nogi, H. Koga, K. Suganuma, M. Hara, E. Nakazawa, H. Uchida, The effect of light and humidity on the stability of silver nanowire transparent electrodes, RSC Adv. 5 (2015) 27657, https://doi.org/10.1039/C5RA02722E.

[21] Y. Ge, X. Duan, M. Zhang, L. Mei, J. Hu, W. Hu, X. Duan, Direct room temperature welding and chemical protection of silver nanowire thin films for high performance transparent conductors, J. Am. Chem. Soc. 140 (2018) 193–199, https://doi.org/10.1021/jacs.7b07851.

[22] Y. Liu, X. Xu, Y. Wei, Y. Chen, M. Gao, Z. Zhang, C. Si, H. Li, X. Ji, J. Liang, Tailoring silver nanowire nanocomposite interfaces to achieve superior stretchability, durability, and stability in transparent conductors, Nano Lett. 22 (2022) 3784–3792, https://doi.org/10.1021/acs.nanolett.2c00876.

[23] X. Zhang, X. Yan, J. Chen, J. Zhao, Large-size graphene microsheets as a protective layer for transparent conductive silver nanowire film heaters, Carbon 69 (2014) 437–443, https://doi.org/10.1016/j.carbon.2013.12.046.

[24] B. Yoo, Y. Kim, C.J. Han, M.S. Oh, J.-W. Kim, Recyclable patterning of silver nanowire percolated network for fabrication of flexible transparent electrode, Appl. Surf. Sci. 429 (2018) 151–157, https://doi.org/10.1016/j.apsusc.2017.07.285.

[25] B. Hwang, P. Matteini, Review of the versatile patterning methods of Ag nanowire electrodes, Coatings 13 (2023) 617, https://doi.org/10.3390/coatings13030617.

[26] J.Y. Song, J.H. Oh, D. Choi, S.M. Park, Highly efficient patterning technique for silver nanowire electrodes by electrospray deposition and its application to self-powered triboelectric tactile sensor, Sci. Rep. 11 (2021) 21437, https://doi.org/10.1038/s41598-021-01043-6.

[27] D.-S. Um, Y. Lee, T. Kim, S. Lim, H. Lee, M. Ha, Z. Khan, S. Kang, M.P. Kim, J. Y. Kim, H. Ko, High-resolution filtration patterning of silver nanowire electrodes for flexible and transparent optoelectronic devices, ACS Appl. Mater. Interfaces 12 (2020) 32154–32162, https://doi.org/10.1021/acsami.0c06851.

[28] I. Jurewicz, A. Fahimi, P.E. Lyons, R.J. Smith, M. Cann, M.L. Large, M. Tian, J. N. Coleman, A.B. Dalton, Insulator-conductor type transitions in graphene-modified silver nanowire networks: a route to inexpensive transparent conductors, Adv. Funct. Mater. 24 (2014) 7580–7587, https://doi.org/10.1002/adfm.201402547.

[29] S.V. Tsygankova, A.A. Chinarev, A.B. Tuzikov, N. Severin, A.A. Kalachev, J. P. Rabe, A.S. Gambaryan, N.V. Bovin, Biantennary oligoglycines and glyco-oligoglycines self-associating in aqueous medium, Beilstein J. Org. Chem. 10 (2014) 1372–1382, https://doi.org/10.3762/bjoc.10.140.

[30] A.B. Tuzikov, A.A. Chinarev, A.S. Gambaryan, V.A. Oleinikov, D.V. Klinov, N. B. Matsko, V.A. Kadykov, M.A. Ermishov, I.V. Demin, V.V. Demin, P.D. Rye, N. V. Bovin, Polyglycine II nanosheets: supramolecular antivirals? ChemBioChem 4 (2003) 147–154, https://doi.org/10.1002/cbic.200390025.

[31] R. Garriga, I. Jurewicz, E. Romero, C. Jarne, V.L. Cebolla, A.B. Dalton, E. Muñoz, Two-dimensional, pH-responsive oligoglycine-based nanocarriers, ACS Appl. Mater. Interfaces 8 (2016) 1913–1921, https://doi.org/10.1021/acsami.5b10077.

[32] R. Garriga, I. Jurewicz, S. Seyedin, N. Bardi, S. Totti, B. Matta-Domjan, E. G. Velliou, M.A. Alkhorayev, V.L. Cebolla, J.M. Razal, A.B. Dalton, E. Muñoz, Multifunctional, biocompatible and pH-responsive carbon nanotube-and graphene oxide/tectomer hybrid composites and coatings, Nanoscale 9 (2017) 7791–7804, https://doi.org/10.1039/C6NR09482A.

[33] R. Garriga, I. Jurewicz, S. Seyedin, M. Tripathi, J.R. Pearson, V.L. Cebolla, A. B. Dalton, J.M. Razal, E. Muñoz, Two-dimensional oligoglycine tectomer adhesives for graphene oxide fiber functionalization, Carbon 147 (2019) 460–475, https://doi.org/10.1016/j.carbon.2019.02.080.

[34] M. Tripathi, R. Garriga, F. Lee, S.P. Ogilvie, A.A. Graf, M.J. Large, P.J. Lynch, K. Papagelis, J. Parthenios, V.L. Cebolla, I. Jurewicz, A.B. Dalton, E. Muñoz, Probing the interaction between 2D materials and oligoglycine tectomers, 2D Mater. 9 (2022) 045033, https://doi.org/10.1088/2053-1583/ac92ec.

[35] M. Domínguez, S. Oliver, R. Garriga, E. Muñoz, V.L. Cebolla, S. de Marcos, J. Galbán, Tectomer-mediated optical nanosensors for tyramine determination, Sensors 23 (2023) 2524, https://doi.org/10.3390/s23052524.

[36] I. Jurewicz, R. Garriga, M.J. Large, J. Burn, N. Bardi, A.A. King, E.G. Velliou, J. F. Watts, S.J. Hinder, E. Muñoz, A.B. Dalton, Functionalization of silver nanowire transparent electrodes with self-assembled 2-dimensional tectomer nanosheets, ACS Appl. Nano Mater. 1 (2018) 3903–3912, https://doi.org/10.1021/acsanm.8b00689.

[37] H.H. Khaligh, I.A. Goldthorpe, Failure of silver nanowire transparent electrodes under current flow, Nanoscale Res. Lett. 8 (2013) 235, https://doi.org/10.1186/1556-276X-8-235.

[38] H.H. Khaligh, L. Xu, A. Khosropour, A. Madeira, M. Romano, C. Pradére, M. Tréguer-Delapierre, L. Servant, M.A. Pope, I.A. Goldthorpe, The Joule heating problem in silver nanowire transparent electrodes, Nanotechnology 28 (2017) 425703, https://doi.org/10.1088/1361-6528/aa7f34.

[39] G. Deignan, I.A. Goldthorpe, The dependence of silver nanowire stability on network composition and processing parameters, RSC Adv. 7 (2017) 35590, https://doi.org/10.1039/c7ra06524h.

[40] Y. Liu, T. He, C. Gao, Surface modification of poly (ethylene terephthalate) via hydrolysis and layer-by-layer assembly of chitosan and chondroitin sulfate to construct cytocompatible layer for human endothelial cells, Colloids Surf. B Biointerfaces 46 (2005) 117–126, https://doi.org/10.1016/j.colsurfb.2005.09.005.

[41] W. Chen, T.J. McCarthy, Chemical surface modification of poly (ethylene terephthalate), Macromolecules 31 (1998) 3648–3655, https://doi.org/10.1021/ma9710601.

[42] N.P. Prorokova, A.V. Khorev, S.Y. Vavilova, Chemical method of surface activation of poly (ethylene terephthalate) fibre materials, Fibre Chem. 41 (2009) 158, https://doi.org/10.1007/s10692-009-9163-5.
[43] S.M. Barlow, R. Raval, Complex organic molecules at metal surfaces: bonding, organisation and chirality, Surf. Sci. Rep. 50 (2003) 201–341, https://doi.org/10.1016/S0167-5729(03)00015-3.
[44] P.M. Claesson, E. Blomberg, J.C. Fröberg, T. Nylander, T. Arnebrant, Protein interactions at solid surfaces, Adv. Colloid Interface Sci. 57 (1995) 161–227, https://doi.org/10.1016/0001-8686(95)00241-H.
[45] S.J. Henley, M. Cann, I. Jurewicz, A.B. Dalton, D. Milne, Laser patterning of transparent conductive metal nanowire coatings: simulation and experiment, Nanoscale 6 (2014) 946–952, https://doi.org/10.1039/C3NR05504C.
[46] C. Mayousse, C. Celle, A. Fraczkiewicz, J.-P. Simonato, Stability of silver nanowire based electrodes under environmental and electrical stresses, Nanoscale 7 (2015) 2107–2115, https://doi.org/10.1039/C4NR06783E.